

Research Note: Overpressure prediction from C-wave seismic data

Robert J. Ferguson^{1*}, Daniel A. Ebrom² and Kimberly M. Kumar³

¹CREWES, Department of Geoscience, University of Calgary, 2500 University Drive NW, Calgary, AB, T2N 1N4, Canada, ²Statoil, Houston, Texas, USA, and ³BP – Columbus Basin, Port of Spain, Trinidad and Tobago

Received January 2010, revision accepted February 2011

ABSTRACT

Recently, mode converted shear waves (C-waves) have been shown to enable overpressure prediction in media where primary wave acquisition is inhibited by gas and fluid effects – C-wave moveout is analysed and a long standing relationship between differential stress and primary-wave (P-wave) velocity is modified and employed. Though pore-pressure prediction based on C-waves is supported by empirical evidence from laboratory and field experiments, a theoretical justification has yet to be developed. In this research note, we provide a supporting algebra for the original relationship between pore pressure and C-wave velocity.

Key words: Converted-wave, Multicomponent, Overpressure, Reservoir geophysics, Velocity analysis.

INTRODUCTION

Drilling safety demands the prediction of anomalous pressure cells and pressure gradients across prior to drilling (Snijder *et al.* 2002). To accomplish this, Eaton (1969) recognizes the advantageous areal extent of reflection seismic data and relates formation pressure gradient and traveltime (obtained from seismic) through the ratio of normally-pressured traveltime Δt_n and observed traveltime Δt_0 . Based on this ratio, Eaton (1969) estimates the overburden stress gradient P/D according to

$$\frac{P}{D} = \frac{S}{D} - \left(\frac{S}{D} - \frac{P}{D_n} \right) \left(\frac{\Delta t_n}{\Delta t_0} \right)^E, \quad (1)$$

where S/D is the overburden stress gradient and P/D_n is the normal pore-pressure gradient. Exponent E is an empirical term determined from sonic transit-time logs obtained from a formation where it is normally pressured and from where it is overpressured (Eaton 1972). With the simple recognition that $\Delta t = \Delta z/\alpha$, where α is the P-wave interval velocity, (Eaton 1972) provided a revised pore-pressure prediction

$$\frac{P}{D} = \frac{S}{D} - \left(\frac{S}{D} - \frac{P}{D_n} \right) \left(\frac{\alpha_0}{\alpha_n} \right)^E, \quad (2)$$

where α_0 is the observed P-wave velocity and α_n is the normally-pressured velocity.

Though pressure prediction based on P-wave data (equation (2)) has seen significant utility (Sayers, Woodward and Bartman 2001), the rather modest reaction of P-waves to pressure change plus the error associated with P-wave velocity estimation drives the search for alternative prediction methods. Kan and Swan (2001) improved velocity estimation based on apparent amplitude variations with offset (AVO). Similarly, Kvam and Landrø (2005) improved velocity estimates based on AVO analysis. Sayers, Johnson and Denyer (2002) used tomography rather than a Dix (1955) approach to velocity estimation. For shale sandstone reservoirs, Carcione *et al.* (2003) use reflection tomography in an inversion scheme where pressure is a fitting parameter.

Ebrom, Heppard and Thomsen (2002) demonstrated that S-waves and C-waves are more sensitive to pressure gradients than P-waves. Before we proceed, however, it is important to remind readers of the uncertainties associated with Eaton (1972) based methods. Eaton (1972) may not be appropriate in regions with strong lateral contrasts in rock and fluid properties due to structural and lithologic variations (Sayers *et al.*

* E-mail: rjfergus@ucalgary.ca

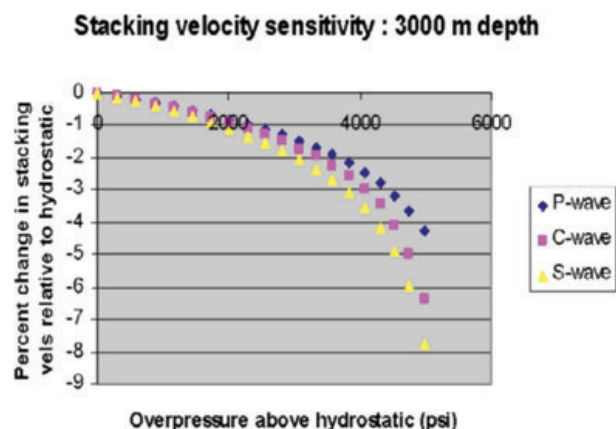


Figure 1 Plot of % change in stacking velocity versus overpressure. For 3000m depth in this numerical experiment, S-waves and C-waves are more sensitive than P-waves.

2001); inversion of velocity for pressure requires prior knowledge of the compaction history of a given region to deconvolve pressure effects from other controls on velocity (Bowers 1999; Ebrom *et al.* 2003; Roberts, Singh and Hornby 2008). Then, there is the major assumption that P-wave stacking velocity has a straightforward relationship with P-wave interval velocity and this is never the case in complex media. As we proceed, we will encounter a further assumption that the ratio of P-wave velocity to shear-wave (S-wave) velocity is constant laterally.

Through numerical experiment, Ebrom *et al.* (2002) showed that, in percent, the change in P-wave stacking velocity is smaller than the change in S-wave and C-wave stacking velocities. As can be seen in Fig. 1, P-wave velocity for a shale zone at 3000 m depth and 4000 psi above hydrostatic pressure, decreases by 2.5 percent where the S-wave and C-wave velocities decrease by 3 and 3.5 respectively. To exploit the larger S-wave response to overpressure, Ebrom *et al.* (2003) adapted Eaton (1975) for S-waves. Experimentally, they found good agreement between their adapted Eaton (1975) equation (2) and the actual pressure curve encountered during drilling¹. Based on S-wave interval velocity obtained from a full-waveform sonic, Ebrom *et al.* (2003) predicted pressure in a formation for comparison to the true pressure encountered. As can be seen in Fig. 2 the calculated curve (blue line) and the true curve (red line) are in good agreement

¹ Because surface mud weight is varied during drilling to prevent blowouts and formation invasion (when under-pressure is encountered), Eaton (1975) used it as a good proxy for the true pressure.

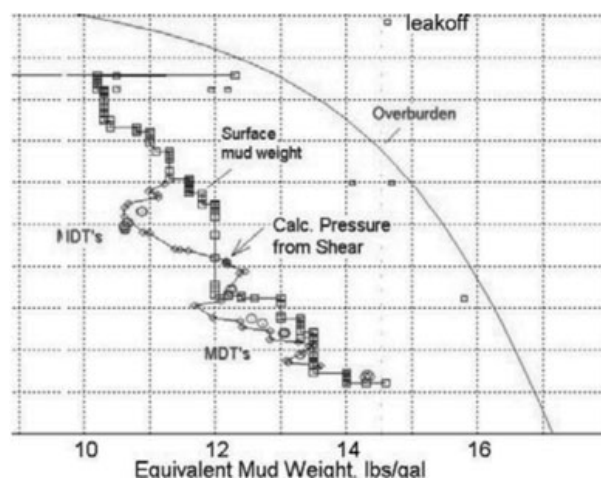


Figure 2 Predicted pressure compared to pressure encountered during drilling. The predicted pressure is based on S-wave interval velocity obtained from dipole sonic logs. Note, the depth axis is omitted for proprietary reasons. Taken from Ebrom *et al.* (2003).

with the exception of a zone between 10.5 and 12 lbs/gal on the mudweight axis (the depth axis is deleted here).

Kumar *et al.* (2006) showed that, where gas clouds exist in the subsurface, mode-converted S-waves (C-waves) provide not only a better image but the resulting stacking velocities are much more reliable; pure P-wave recordings are found to be impacted through bulk modulus due to high gas content, reflection events are discontinuous and interpreted velocities are found to be unreliable. Conversely, Kumar *et al.* (2006) found that C-wave data for the same seismic traverse have reflection events that are much more continuous and the interpreted C-wave stacking velocities (Tessmer and Behle 1988) are found to vary much more slowly and are thought to be more reliable.

Though the procedure is in use in industry, no formal justification of pressure prediction using C-stacking velocity has been presented. In this research note, then, we present a theory to justify this usage. We begin with the basic P-wave based methods for interval velocity (Eaton 1969, 1975) and we invoke the assumption of a laterally invariant ratio of S-wave and P-wave velocity to justify a pressure / S-wave velocity relationship. This assumption is of course violated, for example, at the transition from sediment to salt (Sayers *et al.* 2001). We convert these equations from interval velocity to stacking velocity using a simple argument, and we compute the product of the two results. This product allows us to replace products of P- and S-stacking velocities with C-stacking velocity and provides the desired relationship. Though the use

of C-wave reflections can facilitate pore-pressure prediction where P-waves are weak, we emphasize that C-wave inversion (Ebrom *et al.* 2002, 2003) is based on analogy alone, and that the true relationship between C-waves and pore pressure is much more complicated.

THEORY

Although they provide no formal justification, Ebrom *et al.* (2003) adapted the P-wave method of Eaton (1975) (equation (2)) for use with S-wave interval velocity. Implicitly, Ebrom *et al.* (2003) assumed that the ratios $\alpha_n/\beta_n = \gamma_n$ and $\alpha_0/\beta_0 = \gamma_0$ are constant for the formation, where β_n and β_0 are normally pressured S-wave velocity observed and S-wave velocity respectively. Using this assumption, the ratio $\left(\frac{\alpha_0}{\alpha_n}\right)^E$ in equation (2) becomes

$$\left(\frac{\alpha_0}{\alpha_n}\right)^E = \left(a \frac{\beta_0}{\beta_n}\right)^E = \left(\frac{\beta_0}{\beta_n}\right)^{E+\varepsilon} = \left(\frac{\beta_0}{\beta_n}\right)^{E_\beta}, \quad (3)$$

where $a = \gamma_0/\gamma_n$, E_β is an empirical constant that is determined from S-wave sonic logs, and ε accounts for the difference between E and E_β . Based on S-wave interval velocity, then, equation (2) is given by

$$\frac{P}{D} = \frac{S}{D} - \left(\frac{S}{D} - \frac{P}{D_n}\right) \left(\frac{\beta_0}{\beta_n}\right)^{E_\beta}. \quad (4)$$

For simplicity, Ebrom *et al.* (2003) write equations (2) and (4) in terms of effective pressures $\sigma_{eff,n}$

$$\sigma_{eff,n} = \frac{S}{D} - \frac{P}{D_n}, \quad (5)$$

and

$$\sigma_{eff,0} = \frac{S}{D} - \frac{P}{D}, \quad (6)$$

so that

$$\frac{\sigma_{eff,0}}{\sigma_{eff,n}} = \left(\frac{\alpha_0}{\alpha_n}\right)^E = \left(\frac{\beta_0}{\beta_n}\right)^{E_\beta}. \quad (7)$$

Ebrom *et al.* (2003), for a prospect that they left unspecified, determined a value of $E_\beta = 2$ based on their comparison using surface mud weights and S-wave sonic logs. Ebrom *et al.* (2003) argued that, in the absence of S-wave sonic logs, an alternative to the pressure-velocity relationship of equation (7) may be based on C-wave stacking velocity Kumar *et al.* (2006) provided evidence to support this speculation based on data acquired offshore Trinidad and Tobago. They found that C-wave estimation of pore pressure accurately predicts pore pressures actually encountered in a well bore (Kumar *et al.* 2006).

Our formal support for C-wave prediction of pore pressure begins with the stacking velocities for P-waves and S-waves (Dix 1955 and Appendix A, equations (34) and (35) respectively). Here, equation (7) for a single depth becomes

$$\frac{\sigma_{eff,0}}{\sigma_{eff,n}} = \left(\frac{\tilde{v}_0^\alpha}{\tilde{v}_n^\alpha}\right)^{\tilde{E}} = \left(\frac{\tilde{v}_0^\beta}{\tilde{v}_n^\beta}\right)^{\tilde{E}_\beta}, \quad (8)$$

where \tilde{E} and \tilde{E}_β are new coefficients that correspond to P-wave and S-wave stacking velocities respectively. Though S-wave velocity is a rare measurement, C-stacking velocity is readily available from C-seismic analysis. To derive a pressure equation for C-waves, write

$$\frac{\tilde{v}_{obs}^\alpha}{\tilde{v}_n^\alpha} = \left(\frac{\sigma_{obs}}{\sigma_n}\right)^{\frac{1}{\tilde{E}}}, \quad (9)$$

and

$$\frac{\tilde{v}_{obs}^\beta}{\tilde{v}_n^\beta} = \left(\frac{\sigma_{obs}}{\sigma_n}\right)^{\frac{1}{\tilde{E}_\beta}}, \quad (10)$$

and compute their product

$$\frac{\tilde{v}_{obs}^\alpha \tilde{v}_{obs}^\beta}{\tilde{v}_n^\alpha \tilde{v}_n^\beta} = \left(\frac{\sigma_{obs}}{\sigma_n}\right)^{\frac{1}{\tilde{E}} + \frac{1}{\tilde{E}_\beta}}. \quad (11)$$

Then, from Tessmer and Behle (1988) (Appendix A, equation (37)), $(\tilde{v}^{\alpha\beta})^2 = \tilde{v}^\alpha \tilde{v}^\beta$ and equation (11) become

$$\frac{\tilde{v}_{obs}^{\alpha\beta}}{\tilde{v}_n^{\alpha\beta}} = \left(\frac{\sigma_{obs}}{\sigma_n}\right)^{\frac{1}{2} \left(\frac{1}{\tilde{E}} + \frac{1}{\tilde{E}_\beta}\right)}. \quad (12)$$

The root of equation (12) gives the desired relationship between pressure gradient and C-stacking velocity according to

$$\frac{\sigma_{obs}}{\sigma_n} = \left(\frac{\tilde{v}_{obs}^{\alpha\beta}}{\tilde{v}_n^{\alpha\beta}}\right)^{E_{\alpha\beta}}, \quad (13)$$

where $E_{\alpha\beta} = 2 \frac{E_\alpha E_\beta}{E_\alpha + E_\beta}$ is a new coefficient for C-waves.

In prospects that have significant P-wave attenuation, a value for $E_{\alpha\beta}$ can be computed from the available sonic-log (full waveform) data and mud-weight data. Then, based on C-wave acquisition, and similar to the overpressure prediction methods of Eaton (1975) (P-wave based) and Ebrom *et al.* (2003) (S-wave based), maps of pressure gradient are generated for the entire prospect according to equation (13).

DISCUSSION

There has been a recent explosion in the amount of multicomponent seismic datasets being acquired. For the most part, this increase in multicomponent seismic acquisition has not been

driven by a desire to acquire mode-converted shear-waves. Rather, new MEMS technology has made the acquisition of 3C (or offshore, 4C) seismic data as cheap as single component seismic. The horizontal components are used onshore to predict (and reject) ground roll, thus allowing the cost savings of using individual sensors rather than arrays. Offshore, the horizontal components are used to quantify vector fidelity of individual node plantings.

One consequence of the multicomponent seismic data being acquired for enhanced fidelity of the P-wave signal is that many multicomponent seismic surveys are correctly sampled for P-wave reflections but severely under-sampled for S-wave reflections. A challenge for processing companies is to find some value in the horizontal components of seismic (where the S-wave and C-wave signals are most prominent), rather than just leaving the horizontal component seismic on the shelf, or worse, discarded after the suppression of ground-roll or the calculation of vector fidelity.

A clarification here is that these data sets are under-sampled for C-wave imaging but still contain the moveout information necessary to calculate C-wave velocities. Hence, one utility that these datasets still have is to provide a second source of pressure information. This is of special utility when P-wave reflections are attenuated (Kumar *et al.* 2006). The C-wave velocity pressure estimate can also be important when P-wave velocities have reduced sensitivity to pressure, perhaps due to an unloading mechanism Bowers (2002). Due to the enhanced sensitivity of C-waves to pressure, C-wave velocities can help confirm that small perturbations in P-wave velocity fields are due to pore pressure

CONCLUSIONS

The method of Ebrom *et al.* (2003) that relates differential stress due to anomalous pore pressure and converted-wave velocity is described analytically. The relationship between pure P-wave modes, S-modes and the C-modes is explored in the context of C-wave velocity analysis. The C-wave velocity, rather than being inverted and analysed as a separate mode, is examined as it is and theoretical pore-pressure predictions are made. This approach has advantages in basins where overpressure hazards exist and where gas and fluid effects preclude analysis using P-waves alone. Systematically, this approach is attractive because no specialized software needs to be developed for C-wave velocity analysis or pore pressure prediction. C moveout velocity is simply interpreted as is and only the associated coefficient range differs from the P-wave range.

ACKNOWLEDGEMENTS

The authors wish to thank BP America, the sponsors of EDGER at the University of Texas at Austin and the sponsors of CREWES for their support of this work.

REFERENCES

- Bowers G.L. 1999. Pore pressure estimation from velocity data: Accounting for overpressure mechanisms besides under-compaction. Pore Pressure and Fracture Gradients, SPE Reprint series, 78–84, Society of Petroleum Engineers.
- Bowers G.L. 2002. Detecting high overpressure. *The Leading Edge* 21, 174–177.
- Carcione J.M., Helle H.B., Pham N.H. and Toverud T. 2003. Pore pressure estimation in reservoir rocks from seismic reflection data. *Geophysics* 68, 1569–1579.
- Dix C.H. 1955. Seismic velocities from surface measurements. *Geophysics* 20, 68–86.
- Eaton B.A. 1969. Fracture gradient prediction and its application in oilfield operations. *Journal of Petroleum Technology* 10, 1353–1360.
- Eaton B.A. 1972. Graphical method predicts geopressure worldwide. *World Oil* 182, 51–56.
- Eaton B.A. 1975. The equation for geopressure prediction from well logs. SPE 50th Annual Fall Meeting, Expanded Abstracts, 5544–MS.
- Ebrom D., Heppard P., Mueller M. and Thomsen L. 2003. Pore pressure prediction from S -wave, C -wave, and P -wave velocities. 73rd SEG meeting, Dallas, Texas, USA, Expanded Abstracts, 1370–1373.
- Ebrom D., Heppard P. and Thomsen L. 2002. Numerical modeling of PS moveout as a function of pore pressure. 72nd SEG meeting, Salt Lake City, Utah, USA, Expanded Abstracts, 1634–1637.
- Kan T.K. and Swan H.W. 2001. Geopressure prediction from automatically derived seismic velocities. *Geophysics* 66, 1937–1946.
- Kumar K.M., Ferguson R.J., Ebrom D. and Heppard P. 2006. Pore pressure prediction using an Eaton's approach for PS -waves. 76th SEG meeting, New Orleans, Louisiana, USA, Expanded Abstracts, 1550–1554.
- Kvam O. and Landrø M. 2005. Pore-pressure detection sensitivities tested with time-lapse seismic data. *Geophysics* 70, O39–O50.
- Roberts M.A., Singh S. and Hornby B.E. 2008. Investigation into the use of 2D elastic waveform inversion from look-ahead walk-away vsp surveys. *Geophysical Prospecting* 56, 883–895.
- Sayers C.M., Johnson G.M. and Denyer G. 2002. Pre-drill pore-pressure prediction using seismic data. *Geophysics* 67, 1286–1292.
- Sayers C.M., Woodward M.J. and Bartman R.C. 2001. Pre-drill pore-pressure prediction using 4C seismic data. *The Leading Edge* 20, 1056–1059.
- Snijder J., David Dickson D., Hillier A., Litvin A., Gregory C. and Phil Crookall P. 2002. 3D pore pressure prediction in the Columbus Basin, offshore Trinidad and Tobago. *First Break* 20, 283–286.
- Tessmer G. and Behle A. 1988. Common reflection point data-stacking technique for converted waves. *Geophysical Prospecting* 36, 671–688.

APPENDIX A

This appendix follows closely the paper of Tessmer and Behle (1988) but for additional clarity, we fill in a number of missing steps in that derivation. In general, reflection traveltimes T are hyperboloid functions of offset X

$$T_m^2 = a_m + b_m X_m^2 + c_m X_m^4 \dots, \quad (\text{A1})$$

where, for the n_{th} interface, T_m is the reflection traveltime, X_m source-receiver offset, and +ve powers of X_m ensure +ve traveltimes. For simplicity, assume the relationship is hyperbolic

$$T_m = \sqrt{a_m + b_m X_m^2}. \quad (\text{A2})$$

Estimate a_m and b_m to unravel z_m (thickness of n_{th} layer) and α_m and β_m — P- and S-velocity of the n_{th} layer respectively. Determination of a_m is easy, set $X_m = 0$ to get

$$T_{0,m}^2 = a_m, \quad (\text{A3})$$

where $T_{0,m}$ is the zero-offset traveltime for the m^{th} reflection. This leaves b_m in units of slowness squared (s/m)²

$$b_m = \frac{T_m^2 - T_{0,m}^2}{X_m^2}. \quad (\text{A4})$$

Traveltime from the source to the n^{th} layer is the sum of the P-wave travel times through each layer

$$P_m = \left[P_1 + P_2 + \dots + \frac{z_m}{\alpha_m \cos \theta_m} \right] = \sum_{j=1}^m \frac{z_j}{\alpha_j \cos \theta_j}, \quad (\text{A5})$$

where z_j and θ_j are thickness and angle of refraction through the j^{th} layer respectively and α_j is the corresponding P-wave velocity. Traveltime from the n^{th} layer to a receiver is the sum of the S-wave traveltimes through each layer

$$S_m = \left[S_1 + S_2 + \dots + \frac{z_m}{\beta_m \cos \phi_m} \right] = \sum_{j=1}^m \frac{z_j}{\beta_j \cos \phi_j}, \quad (\text{A6})$$

where ϕ_j is the refraction angle through the j^{th} layer, and β_j is the corresponding S-wave velocity.

Total traveltime T_m for a converted wave reflection from the m^{th} layer is the sum of the P-wave and S-wave traveltimes

$$T_m = P_m + S_m, \quad (\text{A7})$$

or

$$T_m = \sum_{j=1}^m z_j \left[\frac{1}{\alpha_j \cos \theta_j} + \frac{1}{\beta_j \cos \phi_j} \right]. \quad (\text{A8})$$

For general angle ψ and general velocity v , $\cos \psi = \sqrt{1 - \sin^2 \psi}$ and from Snell's Law $\sin^2 \psi = (vp)^2$ where p is

ray parameter. Total traveltime T_m , therefore, becomes

$$T_m = \sum_{j=1}^m z_j \left[\frac{1}{\alpha_j \sqrt{1 - (\alpha_j p)^2}} + \frac{1}{\beta_j \sqrt{1 - (\beta_j p)^2}} \right]. \quad (\text{A9})$$

On the P-wave side, the lateral distance x_j travelled through layer j is:

$$x_j = z_j \tan \theta_j = z_j \frac{\sin \theta_j}{\cos \theta_j} = \frac{\alpha_j z_j p}{\sqrt{1 - (\alpha_j p)^2}}, \quad (\text{A10})$$

and a similar relationship will hold for the S-wave side.

For the m^{th} layer, then, total distance X_m is the sum of distances from the P-wave side and the S-wave side

$$X_m = p \sum_{k=1}^m z_k \left[\frac{\alpha_k}{\sqrt{1 - (\alpha_k p)^2}} + \frac{\beta_k}{\sqrt{1 - (\beta_k p)^2}} \right]. \quad (\text{A11})$$

We want to eliminate dependence on p , so use the series for $[1 + u]^{-\frac{1}{2}}$

$$\frac{1}{\sqrt{1 - (\alpha p)^2}} \approx 1 + \frac{1}{2} (\alpha p)^2. \quad (\text{A12})$$

As shown in Fig. A1, only for $p = 0$ is the approximation exact, with significant departure of the approximate and true curves beyond about 20° angle of incidence. Using the square-root approximation (equation (25)), total traveltime T_m (equation (22)) becomes

$$T_m \approx \sum_{j=1}^m z_j \left\{ \frac{1}{\alpha_j} \left[1 + \frac{1}{2} (\alpha_j p)^2 \right] + \frac{1}{\beta_j} \left[1 + \frac{1}{2} (\beta_j p)^2 \right] \right\}. \quad (\text{A13})$$

Using zero-offset time $T_{0,m} = \sum_{j=1}^m z_j \left[\frac{1}{\alpha_j} + \frac{1}{\beta_j} \right]$, T_m becomes

$$T_m \approx T_{0,m} + \frac{p^2}{2} \sum_{j=1}^m z_j [\alpha_j + \beta_j]. \quad (\text{A14})$$

Similarly, X_m becomes

$$\begin{aligned} X_m &= p \sum_{k=1}^m z_k \left\{ \alpha_k \left[1 + \frac{1}{2} (\alpha_k p)^2 \right] + \beta_k \left[1 + \frac{1}{2} (\beta_k p)^2 \right] \right\} \\ &= p \sum_{k=1}^m z_k [\alpha_k + \beta_k] + \frac{p^2}{2} \sum_{k=1}^m z_k [\alpha_k^3 + \beta_k^3]. \end{aligned} \quad (\text{A15})$$

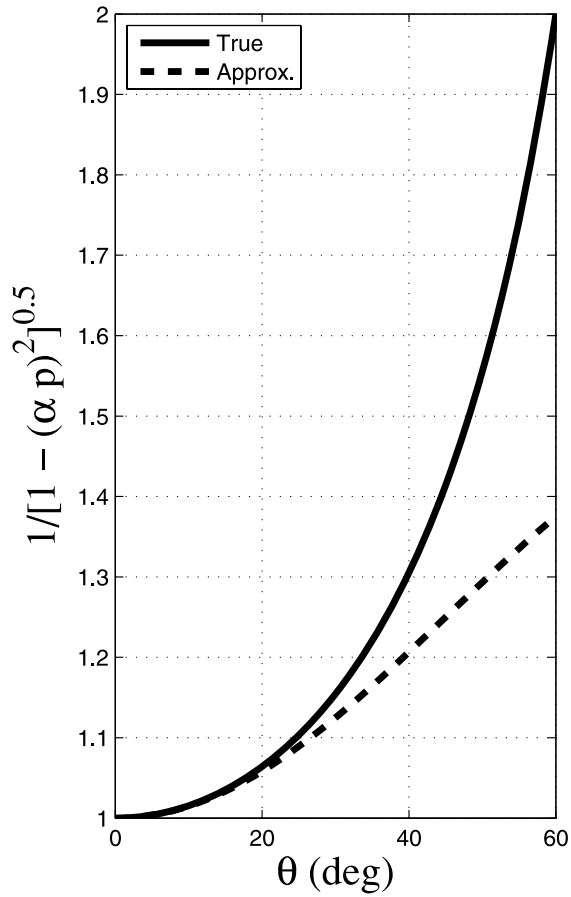


Figure A1 Approximate (true) versus exact curves for $1/\sqrt{1 - (\alpha p)^2}$. The approximate curve departs from the exact curve at $\theta \sim 20$ degrees.

To find b_m , we need T_m^2 and X_m^2 , but we are only keeping powers of p^2 , so T_m^2 and X_m^2 become:

$$T_m^2 \sim T_{0,m}^2 + T_{0,m} p^2 \sum_{j=1}^m z_j [\alpha_j + \beta_j], \quad (A16)$$

and

$$X_m^2 \sim p^2 \left(\sum_{k=1}^m z_k [\alpha_k + \beta_k] \right)^2. \quad (A17)$$

Using T_m^2 and X_m^2 above, b_m becomes

$$b_m \sim T_{0,m} \left(\sum_{k=1}^m z_k [\alpha_k + \beta_k] \right)^{-1} = \frac{\sum_{k=1}^m z_k \left[\frac{1}{\alpha_k} + \frac{1}{\beta_k} \right]}{\sum_{k=1}^m z_k [\alpha_k + \beta_k]} = \frac{\sum_{k=1}^m \left[\frac{1}{\alpha_k} + \frac{1}{\beta_k} \right]}{\sum_{k=1}^m [\alpha_k + \beta_k]}, \quad (A18)$$

where we have used

$$T_{0,m} = \sum_{k=1}^m z_k \left[\frac{1}{\alpha_k} + \frac{1}{\beta_k} \right]. \quad (A19)$$

For each reflector m , b_m is a measurable quantity – it is simply the second coefficient in a hyperbola fit to the m^{th} reflection event. Traveltime $T_{0,m}$ is also measurable – it is the projection to zero-offset of the n^{th} reflection event.

Define the *stacking velocity* for C-waves, then, as

$$(\tilde{v}_m^{\alpha\beta})^2 = \frac{1}{b_k} = \frac{\sum_{k=1}^m \alpha_k \left[1 + \frac{\beta_k}{\alpha_k} \right]}{\sum_{k=1}^m \frac{1}{\alpha_k} \left[1 + \frac{\alpha_k}{\beta_k} \right]}. \quad (A20)$$

Assume now that $\frac{\beta_k}{\alpha_k} = \gamma$ is constant for all k , then $\gamma = \frac{\beta_k}{\alpha_k} = \frac{\tilde{v}_m^\beta}{\tilde{v}_m^\alpha}$ where

$$\tilde{v}_m^\alpha = \sqrt{\frac{\sum_{k=1}^m \alpha_k}{\sum_{k=1}^m \frac{1}{\alpha_k}}}, \quad (A21)$$

and

$$\tilde{v}_m^\beta = \sqrt{\frac{\sum_{k=1}^m \beta_k}{\sum_{k=1}^m \frac{1}{\beta_k}}}, \quad (A22)$$

are stacking velocities for P-waves and S-waves respectively, and write equation (33) in terms of γ as

$$(\tilde{v}_m^{\alpha\beta})^2 = \frac{1 + \gamma \sum_{k=1}^m \alpha_k}{1 + \frac{1}{\gamma} \sum_{k=1}^m \frac{1}{\alpha_k}} = \gamma \frac{\sum_{k=1}^m \alpha_k}{\sum_{k=1}^m \frac{1}{\alpha_k}}. \quad (A23)$$

Recognizing $(\tilde{v}_m^p)^2$ in the second term of equation (36) we have

$$(\tilde{v}_m^{\alpha\beta})^2 = \gamma (\tilde{v}_m^\alpha)^2 = \frac{\tilde{v}_m^\beta}{\tilde{v}_m^\alpha} (\tilde{v}_m^\alpha)^2 = \tilde{v}_m^\beta \tilde{v}_m^\alpha. \quad (A24)$$

Equation (37) is used in the body of this research note to convert the P-wave and S-wave estimation of pore pressure to an estimate that is based on C-wave stacking velocity.